A&A 391, 967–978 (2002)
DOI: 10.1051/0004-6361:20020983
© ESO 2002

Astronomy & Astrophysics

H_2O and SiO maser emission in Galactic center OH/IR stars⋆,⋆⋆

L. O. Sjouwerman[1,2,3], M. Lindqvist[1], H. J. van Langevelde[2], and P. J. Diamond[3,4]

[1] Onsala Space Observatory, 439 92 Onsala, Sweden
[2] Joint Institute for VLBI in Europe, Radiosterrenwacht, PO Box 2, 7990 AA Dwingeloo, The Netherlands
[3] N.R.A.O. Array Operations Center, PO Box 0, Socorro, NM 87801, USA
[4] MERLIN/VLBI National Facility, Jodrell Bank Observatory, Macclesfield, Cheshire SK11 9DL, UK

Received 15 July 1999 / Accepted 6 March 2002

Abstract. We have performed targeted surveys for 22 GHz H_2O and 43 GHz SiO maser emission in Galactic center OH/IR stars using the Very Large Array. Some of the detections have been used in a previous paper to investigate the possibility of measuring milli-arcsecond accurate positions (to obtain stellar proper motions) in the Galactic center. Here we report on the detection of at least 25 H_2O masers and 18 SiO masers associated with stars within 2° and 15′ of Sgr A*, respectively. This survey has more than doubled the total number of proper motion candidates to at least about 50 stellar objects. The stellar SiO masers are best suited for proper motion studies, although the initial OH, H_2O or SiO maser positions may not be well enough determined to use for a-priori VLBI positions. Serendipitously we also found 8 H_2O masers in the molecular cloud M−0.13−0.08.

Key words. masers – surveys – astrometry – stars: AGB and post-AGB – galaxy: center

1. Introduction

The dynamics of the central (∼50 pc) region of the Galaxy still poses some interesting questions. The mass distribution, in particular the question whether Sgr A* is a massive black hole, is the most intriguing issue. Outside the immediate ∼10 pc scale environment of Sgr A*, observations provide evidence for a "bar", and/or a tri-axial bulge. In the past decade many studies to probe the inner Galactic gravitational potential have been performed, using line-of-sight velocities of gas and stars (e.g. Blitz et al. 1993; Genzel et al. 1994; Morris & Serabyn 1996; Mezger et al. 1996). However, in this part of the Galaxy interstellar gas is an unreliable probe to sample the local velocity field, because it might be subject to non-gravitational forces such as stellar winds, radiation pressure and magnetic fields. Also, gas may be transported inward on non-circular motions by a barred potential.

Stellar objects make much better test particles, because they are less susceptible to non-gravitational forces. To improve the present situation, we plan to measure transverse velocities of OH/IR stars in the Galactic center (GC) found by Lindqvist et al. (1992; for further reading on asymptotic giant branch (AGB) and OH/IR stars we recommend Habing 1996 or Iben 1991). All these OH/IR stars observed toward Sgr A* appear to be located in the GC, at an adopted distance of 8 kpc (Reid 1993). But because of severe interstellar scattering toward the GC (van Langevelde et al. 1992b; Frail et al. 1994), the 1612 MHz OH masers are not useful. The higher frequency 22 GHz H_2O and 43 GHz SiO masers, known to reside frequently in OH/IR stars, are more favorable since scattering scales as ν^{-2}. However, so far few surveys for H_2O and SiO masers in the GC have been performed, limiting the number of candidate objects for a proper motion survey. Early targeted single dish observations (Lindqvist et al. 1990; Lindqvist et al. 1991) resulted in 15 high frequency stellar proper motion candidates. More recently additional individual stars with H_2O and SiO masers have become available (e.g. Levine et al. 1995; Menten et al. 1997; Miyazaki et al. 2001; Deguchi et al. 2002), however the number of stellar proper motion candidates was increased by only a handful[1].

We have performed a targeted search for H_2O and SiO maser emission in OH/IR stars in the GC with the Very Large Array (VLA) to obtain a larger sample of proper motion candidates. We describe the observations in Sect. 2, and the data reduction in Sect. 3. We identify the stellar H_2O and SiO masers, and the H_2O masers associated with star forming regions (SFR's) among our detections in Sect. 4. In Sect. 5, we comment on some aspects of positions and variability. We conclude with the number of proper motion candidates; a first report on measuring their positions with the Very Long

Send offprint requests to: L. O. Sjouwerman (Socorro),
e-mail: lsjouwerm@nrao.edu

⋆ Figures 1 to 4 are only available in electronic form at http://www.edpsciences.org

⋆⋆ Tables 2–4 are also available in electronic form at the CDS via anonymous ftp to cdsarc.u-strasbg.fr (130.79.128.5) or via http://cdsweb.u-strasbg.fr/cgi-bin/qcat?J/A+A/391/967

[1] During the final stages of the publication of this paper, Imai et al. (2002 PASJ 54, L19) published a list of 79 43 GHz SiO masers, extending the list presented here considerably.

Table 1. Observational summary.

Set	Date	$\nu_{\rm rest}$	Array	Mode	BW	Δv	Resolution	1733−130	Sgr A*	rms	Number	
		GHz			MHz	kHz	$'' \times '' \times$ km s^{-1}	Jy	Jy	[a]	obs'd	det'd
(1)	(2)	(3)	(4)	(5)	(6)	(7)	(8)	(9)	(10)	(11)	(12)	(13)
						H_2O maser surveys:						
1a	6 Jul. 93	22.235	C	2AC	6.25	97.7	$2.5 \times 1.9 \times 1.3$	4.6	(0.3)[b]	15	153	21+9
1b	8 Jul. 93							4.0	0.7			
1c	10 Jul. 93							4.2	0.7			
2a	20 May 94	22.235	A[1]	2BD	6.25	97.7	$0.3 \times 0.2 \times 1.3$	6.1	0.9	10	19	8+1
3a	2 Jun. 94		BnA[1]					5.1	0.9	-	17	-
						SiO maser surveys:						
2b	20 May 94	42.820	A[2]	2AC	12.50	390.6	$1.6 \times 0.7 \times 2.8$	9[c]	1.4	60	25	6
3b	2 Jun. 94		BnA[2]		6.25	97.7	$\times 0.7$	9[c]	1.5	-	23	-
4a	29 Jan. 95	42.820	DnC[3]	2AC	6.25	195.3	$4.3 \times 2.0 \times 1.4$	9[c]	1.1	15	19	15*
4b		43.122		2BD				9[c]	1.1			15*

[1] 17 antennas on the outer stations of the configuration.
[2] 9 antennas on the inner three stations along each arm.
[3] 9 antennas with 43 GHz receivers put in a spiral pattern.
[a] Typical rms noise level in mJy beam^{-1}.
[b] On July 8, source J1744−312 instead of Sgr A*.
[c] Adopted 43 GHz flux density for J1733−130.
* A total of 16 sources: 14 sources are detected in both the ($v = 1$) and ($v = 2$) lines; a 15th source in this one line only.

Baseline Array (VLBA) can be found in Sjouwerman et al. (1998a). With Sgr A* as phase reference, the new dual-beam Japanese VLBI Exploration of Radio Astrometry (VERA) network (e.g. Hachisuka 2000; Honma et al. 2000) will probably be the preferred instrument to follow up the Sjouwerman et al. (1998a) VLBA efforts with the masers presented in this paper.

The OH names and OH positions used throughout this paper are taken from Lindqvist et al. (1992) unless stated otherwise. Velocities in this paper refer to line-of-sight velocities with respect to the Local Standard of Rest (LSR).

2. Observations

In this section we first present the chronology of the observations. The second part of this section contains general comments on the calibration. In 1993, our initial aim was to detect H_2O masers associated with the OH/IR stars with positions accurate enough for follow up VLBI observations; i.e. better than the $1''$ to $2''$ accurate OH positions available. In 1994 we searched for both H_2O and SiO maser emission. During the course of the project, our focus shifted from 22 GHz H_2O masers to 43 GHz SiO masers, because it became clear that SiO masers were a better prospect for obtaining candidates. This is partly because the higher frequency of the SiO maser allows measurements at higher resolution, but moreover because the SiO maser line generally shows less capricious behavior than H_2O. Finally, after deciding to use only SiO masers for our proper motion campaign, in 1995 we searched for the ($v = 2$), as well as for the ($v = 1$) line.

2.1. Observational history

In July 1993 we used the VLA to search for 22 GHz H_2O masers in the 153 1612 MHz OH masers, most of them associated with OH/IR stars, that were known in the GC at that time[2] from a survey by Lindqvist et al. (1992). The details of these observations, and those of subsequent observations, can be found in the left hand columns of Table 1. Listed are a data set code (1) corresponding to an observing date (2) and rest frequency of the maser line (3), the array configuration (4) and the correlator mode (5), the total bandwidth (6) and channel separation (7).

In 1993 the observing setup was such that phases were calibrated every 15 min; the time on-source was 5 min. With only a few detections (and an unfortunate calibrator choice), a very low detection rate was obtained. Apart from bad weather, this is possibly also due to the variable nature of the H_2O masers. We concluded that we did not have enough H_2O masers for a proper motion campaign.

In the beginning of 1994, a number of VLA antennas were equipped with 43 GHz receivers, enabling us to search for SiO masers in the OH/IR stars. We selected 48 OH/IR stars from the sample of Lindqvist et al. (1992) which were located within $15'$ of Sgr A*. In May and June 1994 they were observed at 43 GHz in a search for ($J = 1 \rightarrow 0$, $v = 2$) SiO maser emission. At the same time, a similar sample was searched at 22 GHz for H_2O masers as well. The VLA was divided into two sub-arrays: one sub-array with the 43 GHz receivers on the VLA antennas located on the "inner arms", and another sub-array with the other ("outer arm") antennas observing at 22 GHz.

The phase calibration at 22 GHz was performed every 30 (or 15) min with an on-source time of typically 14 min. The H_2O maser detection rate was much higher on May 20 (≈50%). However, we also encountered broad-band

[2] For a compilation of the data, see the Appendix in Sjouwerman et al. (1998b) which also includes more than 50 additional OH/IR stars in the central $35'$ (80 pc) of the GC.

interference hindering us in the bandpass calibration of the June 2 observations; these data were discarded. As this was also the case for the 43 GHz measurements of this day, we presume the interference was generated locally.

For the 43 GHz observations we integrated for 6 min on each source and calibrated the phase between source switches. Six sources were detected on May 20 (Fig. 1). Much of the data was lost, however, because of poor phase stability over the relatively long integration time and large array configuration. Phases were stable in several one to three minute intervals, but changed rapidly in between. Visibility averaging or mapping the source did not yield many results. However, with a self-calibration scheme (Sect. 3.2) we found hints that several OH/IR stars indeed had detectable SiO masers. Because of an unreliable bandpass calibration (mentioned in the previous paragraph) in addition to the rapid atmospheric phase fluctuations, the June 2 measurements did not yield any results from direct imaging with, or without bandpass calibration.

In January 1995 we re-observed 19 OH/IR stars, this time searching for SiO maser emission only. The 19 objects were subjectively selected from the observations in 1994 (Sect. 3.2). We observed simultaneously in the 43 GHz ($J = 1 \rightarrow 0,\ v = 1$) and ($J = 1 \rightarrow 0,\ v = 2$) transitions. In 1994 we chose only the ($v = 2$) transition of SiO, because it is generally the stronger one in OH/IR stars (Nyman et al. 1986, 1993; Lindqvist et al. 1991). With half the calibration cycle of the 1994 observations and 7 min on-source, we obtained a relatively high detection rate (in this subjectively selected sample well over 75%). During these observations the VLA was in its most compact array configuration, with the 43 GHz receivers arranged in a "spiral configuration" and not on the "inner" three antennas on each arm as had been the practice before.

2.2. Calibrator sources

On July 7 1993 we used J1744−312 as a phase calibrator, but we noted that it was too weak at 22 GHz. In subsequent observations at 22 as well as at 43 GHz, we chose Sgr A* as phase calibrator (at a J2000 position of $\alpha = 17^{\rm h}45^{\rm m}40\overset{\rm s}{.}0850$, $\delta = -29^\circ00'27\overset{''}{.}790$), despite the extended background radiation of the Sgr A complex. The extended background was mostly resolved out by the array configuration; all baselines longer than 25 and 20 kλ are usable for 22 and 43 GHz, respectively.

The first and last observing sequence of 3 targets for each observing day in July 1993 could only be referenced to one calibrator scan, i.e. the visibility phases for these targets had to be extrapolated, possibly introducing some positional inaccuracies. All target sources in the May 1994 and January 1995 observations were enclosed by the phase calibrator Sgr A*, which allowed all visibility phases on the target sources to be interpolated.

For all observations we used J1733−130 for bandpass calibration, which for the 43 GHz observations were preceded by pointing scans on J1733−130 taken every one or two hours. For the 22 GHz observations we included J1331+305 for absolute flux calibration. An accurate flux determination at 43 GHz was complicated by the fact that we used the new VLA 43 GHz receivers before a proper calibration had been done. With an adopted 43 GHz flux for J1733-130 (of 9 ± 3 Jy, VLA test memo #192), we determined fluxes for Sgr A* as shown in Col. 10 of Table 1. From the fluxes we derive for Sgr A* with this assumption, we expect that the approximate fluxes do not deviate more than 30% from the true values, although we note that Bower et al. (1997) do report an increase in flux for J1733−130 during the interval between the observations. This indicates that our measured fluxes for January 1995 are lower limits. For future reference, we measured a flux of 0.49 ± 0.03 Jy for the amplitude calibrator J0137+331 in January 1995 (J1331+305 could not be observed).

3. Data reduction

All data sets were calibrated according to a standard spectral line calibration scheme with the NRAO AIPS package. Because of problems determining a bandpass calibration, we quickly scanned the 2 June 1994 22 and 43 GHz data sets for strong masers in the autocorrelation spectra before we had to regard the data as not usable. For all the other data sets, we made image cubes of about 25″ in diameter around the OH maser positions. In cases where we pointed the telescopes such that more than one OH/IR star would fall in the primary beam (and velocity coverage), we chose to image the full primary beam (2′ or 1′ for 22 and 43 GHz respectively) which is less troublesome than to image each position separately. For these larger image cubes, we searched the OH/IR star positions and also detected several H_2O masers serendipitously. Below we will only pay some attention to our serendipitous detections of OH359.956−0.050, and the H_2O masers in the molecular cloud M−0.13−0.08. A summary of the image cubes can be found in Table 1, where we give the spatial and spectral resolution of the image cubes (8), the measured fluxes for our calibrators (9), (10), a representative value for the noise in the image cube (11), the total number of fields searched for emission (12) and the number of detections in OH/IR stars + tentative associations with OH/IR stars in those fields (13).

3.1. H_2O maser profiles

Many studies of H_2O masers in different types of objects have been performed in collections of late-type stars with circumstellar environments originating from mass-loss of the central object: a mixture of supergiants, semi-regular variable stars, Mira and OH/IR stars (Olnon et al. 1980; Engels et al. 1986, 1988; Nyman et al. 1986, 1993 and Engels & Lewis 1996; see also the compilation of other objects in Comoretto et al. 1990; Brand et al. 1994). From these studies, a distinction between the different types of stars, and star forming regions, may be made based on the characteristics of the H_2O and OH maser emission. However, the classification scheme is valid in a statistical sense, and thus not watertight, in particular in the GC where helpful additional optical or infrared information is difficult to obtain.

For OH/IR stars, Engels et al. (1986) divided the H_2O maser detections into two types, A and B, characterized by their spectral shape. Olnon et al. (1980) have proposed

a similar sub-division using several OH maser lines for different types of late-type variable stars. Type A masers show a single H_2O maser peak close to the systemic velocity; type B H_2O masers are double peaked and usually symmetric around the mean, systemic velocity. Most of the type B H_2O maser have a smaller velocity separation between the H_2O maser peaks than the 1612 MHz OH maser, although occasionally the H_2O maser separation is a few km s^{-1} larger compared to OH. Whether a source shows an A or B (or A/B, Engels & Lewis 1996) type H_2O maser is strongly dependent on the IRAS colors of the source; blue Miras predominantly show type A, red OH/IR stars mainly type B spectra (Engels & Lewis 1996). The variability of the maser is reflected in the peak flux density of the emission at fixed velocities; not in changing velocity profiles (with a reservation for rare sources that show mode switching; Engels et al. 1997). In our search for detections we were helped by these characterizations and the knowledge of the 1612 MHz OH profiles. Most of our H_2O maser detections toward the OH maser sources can be characterized as type A or type B H_2O masers. Because of sensitivity limits, we often find only one (the dominant) peak of a B-type double peaked H_2O maser profile, and also in our sample the blue shifted peak is in a statistical sense more dominant than the red shifted one (see discussion in Engels & Lewis 1996). Supergiants, OB star associations and star forming regions are known to have much more complex, and changing H_2O (and OH) maser spectral profiles (e.g. Engels et al. 1988; Genzel & Downes 1977; Genzel & Downes 1979; Reid et al. 1988; Engels & Lewis 1996). Probably typical examples of such SFR's in this survey are sources OH359.751−0.371 and OH359.936−0.144.

3.2. SiO maser profiles; self-calibration

Inspection of the 43 GHz image cubes of the 20 May 1994 observations yielded 6 clear SiO maser detections out of 25 within the positional accuracy (1″) and at about the stellar velocity derived from the OH maser (Fig. 1). From Lindqvist et al. (1992) and Sjouwerman et al. (1998b) we have OH positions accurate to ∼1″. Here we used the positions from Lindqvist et al. (1992) because the survey was done before the Sjouwerman et al. (1998b) survey was finalized; see also Sect. 5.1. However, some tentative and weak SiO masers deviate considerably (up to 10″) from these OH positions. We think these positional differences are due to phase calibration problems. In many of the image cubes we found channels with emission exceeding the noise. We believe that the emission is real since we had problems with the phase calibration. Analyzing the data of the reliable detections, we could see that the visibility phases were stable over several one minute scans, but could switch more than a radian in the next minute. Using knowledge on the spectral profile of SiO masers, we attempted to image more sources, or at least to obtain candidates for re-observation. In doing this we made use of the fact that SiO emission is found around the stellar velocity (the mean of the OH maser peaks) and usually has a width of about 5 km s^{-1}, in our data thus a few channels wide (e.g. Nyman et al. 1986; Lindqvist et al. 1991). Furthermore, we assume the noise in individual, uniformly weighted frequency channels to be mostly independent and take the interval of atmospheric phase stability to be one minute.

Assuming that a certain channel covers a part of the broad SiO maser profile, we self-calibrated the data from this channel assuming a point source model. The self-calibration solution was then applied to all channels. Now, if the channel does not contain line emission, noise in this channel will add up into a spurious detection. However, because the noise in each channel is independent, the solution for this channel applied to the next channels will not yield a similar addition of noise there, thereby yielding no significant systematic emission at this location in the adjacent channels.

However, we found many sources – also in the "unusable" 43 GHz June 1994 observations – for which a solution for one frequency channel aligned flux in several consecutive channels. We regarded such sources as worthy of further investigation and their names were collected for the re-observation program. Because of the extra contribution of the noise in one channel and a missing bandpass calibration for the June 2 data set, spectral profiles and fluxes are not determined for these sources. A chance alignment of another source with the same line-of-sight velocity in the primary beam, other than the source we pointed at, seems unlikely but cannot be excluded. However, the justification of the method is shown by the successful detection of almost all of these re-observed sources in January 1995. For the H_2O masers, the spectral profile is much less regular and many maser spots are spectrally unresolved in our data sets. Hence, the scheme outlined above unfortunately does not work properly for the H_2O masers.

4. Results

In summary we have 25 H_2O maser detections in OH/IR stars, 2 H_2O maser detections in SFR's, and 10 H_2O masers tentatively associated with OH/IR stars (see below). We have also detected 18 SiO masers in OH/IR stars. The H_2O maser detections associated with the OH sources are given in Table 2 and Fig. 2, H_2O masers associated with the molecular cloud M−0.13−0.08 in Table 3 and Fig. 3, and the SiO maser detections in OH/IR stars in Table 4 and Figs. 1 and 4. The clear non-detections and non-redetections are summarized in Table 5.

All detections, in Tables 2–4, have entries for the name of the source in Galactic coordinates (1), the code of the data set (2) and the position in J2000 coordinates (3), (4), with either the offset (Δ) from the original OH position (5), (Tables 2 and 4), or the maximum of the formal error in either RA or Dec. in arcseconds (ϵ) as measured with the AIPS task IMFIT (5), (Table 3). In Table 2 we added the velocity range of the OH maser (6), (7), for comparison with the H_2O maser velocities. The OH maser velocity range is also indicated in the spectra in Fig. 2 by vertical dashed lines. Furthermore, for the H_2O masers in Tables 2 and 3, we list the velocity of the associated most blue shifted (8), the central (9), and the most red shifted (10) components (where appropriate), the highest peak flux of the profile (11), and the total (spatially and spectrally) integrated line flux (12). An asterisk after the OH name for the H_2O maser in Table 2

Table 2. H_2O maser detections in targeted 1612 MHz OH masers in the Galactic center.

OH Name	Set	H_2O Position (J2000)		Δ	Range V_{OH}		V_{blue}		V_{red}	S_{peak}	I_{total} [a]
		RA	Dec	$''$	km s^{-1}		km s^{-1}			Jy	
(1)	(2)	(3)	(4)	(5)	(6)	(7)	(8)	(9)	(10)	(11)	(12)
359.429+0.035*	1a	17 44 7.372	−29 24 7.65	10.72	−10.8	17.6	−0.6			0.50	0.74
359.487+0.081*	1a	17 44 4.098	−29 19 54.90	7.74	−70.9	−30.1	−74.2	−47.9		0.30	0.59
359.508+0.179*	1b	17 43 45.624	−29 15 34.86	14.58	−139.9	−100.2	−134.5		−98.9	0.25	0.56
359.513+0.174	1c	17 43 46.772	−29 15 37.83	1.02	109.2	129.7	114.2			0.23	0.95
359.517+0.001	1a	17 44 27.655	−29 20 48.63	2.33	−145.6	−111.5	−146.9		−111.4	0.22	0.44
359.712−0.263	1c	17 45 57.566	−29 19 9.81	0.17		−5.1		−17.0	−7.7	0.35	1.08
359.745−0.404	1b	17 46 35.629	−29 21 49.68	2.28	169.4	203.5	173.3			0.18	0.56
359.751−0.371†	1b	17 46 28.712	−29 20 29.16	1.36		−8.5	−25.6		−9.8	1.05	7.95
359.760+0.072	1c	17 44 45.989	−29 6 13.86	0.59	−76.3	−34.6	−73.3			0.14	0.75
359.765+0.082	1c	17 44 44.517	−29 5 40.17	3.11	95.6	127.4	93.1	107.6		0.17	1.69
359.768−0.207	1a	17 45 52.676	−29 14 33.29	2.57	−173.9	−135.4	−169.1		−136.2	0.08	0.28
359.783−0.392	1a	17 46 38.348	−29 19 24.66	6.97	194.4	221.0		209.0	226.1	0.10	0.12
359.837+0.120	1a	17 44 45.842	−29 0 42.59	2.49	−374	−336		−341.8		0.09	0.39
359.855−0.078	1a	17 45 34.734	−29 6 2.70	1.01	−18.7	25.5	−8.4		21.8	0.16	2.03
359.897−0.065	2a	17 45 38.396	−29 3 35.83	5.92	−154	−126		−132.1		0.08	0.15
359.906−0.041	2a	17 45 33.528	−29 2 16.24	0.51	−161.4	−121.7	−156.0		−125.7	0.63	1.96
359.924+0.034*	1c	17 45 18.961	−28 58 56.94	5.61	−94.5	−72.1	−92.5			0.17	0.53
359.936−0.144†	1b	17 46 1.966	−29 3 58.78	1.32		−11.9		−13.2		1.52	9.47
,,	2a	1.969	58.48	1.00		,,		−19.8		1.88	5.76
359.943+0.260	1a	17 44 28.035	−28 50 49.08	7.54	−202.3	−168.3	−202.4			0.10	0.44
359.946−0.047	2a	17 45 40.674	−29 0 23.51	0.74	−47.1	−7.4	−44.3			0.46	0.93
359.956−0.050	1c	17 45 42.749	−28 59 56.83	1.31	34.2	66.2	44.8			0.35	1.44
,,	2a	42.763	57.20	1.24	,,	,,	43.5		56.7	0.16	0.62
359.970−0.049	2a	17 45 44.356	−28 59 12.99	0.26	37.5	94.5			92.2	0.07	0.31
359.971−0.119	2a	17 46 0.990	−29 1 23.04	0.57	−27.8	10.8	−23.0		4.7	0.09	0.35
0.040−0.056	2a	17 45 56.127	−28 55 51.71	0.47	50.5	92.2	56.9			0.24	0.77
0.060−0.018*	2a	17 45 49.244	−28 53 29.43	12.93	−23.3	15.3		−1.4	15.7	0.06	0.12
0.071+0.127	1c	17 45 17.635	−28 48 36.46	1.00	−55.0	−17.6	−52.8			0.20	0.36
0.071−0.205	1a	17 46 35.720	−28 58 58.39	5.15	99.0	126.3		110.1	128.5	0.10	0.10
0.076+0.146	1b	17 45 13.876	−28 47 42.05	1.77	0.6	42.6	5.8		33.5	0.09	0.63
0.134−0.023*	1c	17 46 1.417	−28 50 6.57	6.31	−41.4	0.6	−40.2			0.18	0.60
0.142+0.026*	1b	17 45 52.255	−28 48 14.11	13.71	0.6	47.1	2.8	25.2	48.9	0.12	0.32
0.178−0.055*	1a	17 46 15.825	−28 48 35.62	13.61	−52.8	−19.9	−48.8		−23.7	0.11	0.46
0.190+0.036*	1a	17 45 55.315	−28 45 27.21	10.72	144.4	173.9	143.4			0.11	0.19
0.349+0.053*	1c	17 46 14.959	−28 36 46.92	9.08	17.6	46.0		39.7		0.29	0.47
0.379+0.159	1a	17 45 54.059	−28 31 45.20	3.54	124.0	154.6	127.4	139.3	153.8	0.12	0.24
0.543−0.043	1b	17 47 4.897	−28 29 39.78	4.29	−23.3	16.5	−16.6			1.20	5.41
0.548−0.059	1c	17 47 9.076	−28 29 51.65	4.75	−64.1	−0.5			−16.5	0.40	0.63
0.589−0.108	1c	17 47 25.633	−28 29 20.65	7.89	−214.8	−185.3		−202.6	−189.5	0.32	0.87

* Tentative association; see discussion in Sect. 3 and 4.

† SFR, not stellar (OH/IR); see discussion in Sect. 4.1.

[a] Units in Jy km s^{-1}.

indicates whether the measurements concern tentative associations. Table 4 is completed by listing the mean velocity (6), (9), the highest peak flux (7), (10), and the total integrated line flux (8), (11) for the (v = 2), and for the (v = 1) transition respectively. We chose the position with the smallest formal error; (v = 2) if "Set" in Col. 2 lists "2b" or "4a", (v = 1) for "Set" equal to "4b"; they are however consistent with each other to the sub-arcsecond level. The spectra for all detections can be found in Figs. 1–4.

As the initial OH positions have an accuracy of 1–2$''$ (Lindqvist et al. 1992; van Langevelde et al. 1992a; Habing et al. 1983; Sjouwerman & van Langevelde 1996),

Table 3. Serendipitous H_2O maser detections in M−0.13−0.08.

H_2O Name	Set	Position (J2000)		ϵ	V_{blue}	$V_{central}$	V_{red}	S_{peak}	I_{total}	Note
		RA	Dec	$''$		km s^{-1}		Jy	Jy km s^{-1}	
(1)	(2)	(3)	(4)	(5)	(8)	(9)	(10)	(11)	(12)	
359.859−0.079	2a	17 45 35.461	−29 5 47.86	0.021		12.6		0.28	0.48	
359.861−0.082	1a	17 45 36.297	−29 5 49.63	0.077		8.7		0.25	1.85	
861−0.082	2a	36.377	49.16	0.028		10.0		0.31	1.80	
359.864−0.084	1a	17 45 37.458	−29 5 44.28	0.093	4.7		11.3	0.14	0.77	
359.864−0.083	2a	17 45 37.214	−29 5 41.48	0.040		10.0		0.13	0.33	
359.864−0.084	1a	17 45 37.527	−29 5 42.83	0.124		3.4		0.12	1.48	
359.864−0.085	2a	17 45 37.676	−29 5 43.80	0.015		28.4		0.41	0.87	Star? Sect. 4.1
359.865−0.085	1a	17 45 37.832	−29 5 42.88	0.062	−17.7		−8.4	0.95	6.91	
865−0.085	2a	37.917	42.64	0.019	−13.7		−7.1	0.29	1.22	
359.874−0.079	1a	17 45 37.754	−29 5 2.99	0.043		−13.7		0.15	0.98	

Table 4. SiO maser detections in OH/IR stars in the Galactic center.

					(v = 2), 42.820 GHz			(v = 1), 43.122 GHz		
OH Name	Set	SiO Position (J2000)		Δ	V_{system}	S_{peak}	I_{total}	V_{system}	S_{peak}	I_{total}
		RA	Dec	$''$	km s^{-1}	Jy	Jy km s^{-1}	km s^{-1}	Jy	Jy km s^{-1}
(1)	(2)	(3)	(4)	(5)	(6)	(7)	(8)	(9)	(10)	(11)
359.763−0.042	4b	17 45 13.069	−29 9 34.99	1.04	122.7	0.17	0.25	122.7	0.19	0.61
359.765+0.082	4b	17 44 44.460	−29 5 37.33	0.37	111.5	0.62	2.87	111.5	0.97	4.05
359.778+0.010	4a	17 45 3.244	−29 7 12.35	0.29	−28.4	0.50	1.47	−28.4	0.58	1.47
359.803−0.021	4a	17 45 13.928	−29 6 55.17	1.91	−16.3	0.75	3.79	−15.0	0.31	1.84
359.810−0.070	4a	17 45 26.401	−29 8 2.30	1.96	−36.6	0.29	1.58	−33.9	0.22	1.11
359.855−0.078	4b	17 45 34.769	−29 6 3.14	1.01	4.0	0.41	2.62	4.0	0.38	1.76
359.946−0.047	4b	17 45 40.639	−29 0 24.10	0.22	−27.3	0.37	3.47	−27.3	0.44	2.96
359.952−0.036	4a	17 45 38.676	−28 59 45.57	0.55	84.9	0.19	0.27	84.9	0.28	1.21
359.954−0.041	4a	17 45 40.250	−28 59 46.86	1.37	69.9	0.29	1.33	71.3	0.19	1.64
359.971−0.119	4a	17 46 0.967	−29 1 22.77	0.51	−8.5	2.13	9.87	−9.9	0.47	1.72
359.974+0.162	4a	17 44 55.639	−28 52 26.21	0.77	27.7	0.57	2.24	27.7	0.51	3.38
359.977−0.087	2b	17 45 54.368	−29 0 2.66	0.17	10.8*	0.70*	3.80*	not detected in Jan. 95		
359.996−0.144	4b	17 46 10.413	−29 0 51.17	2.41	-	-	-	−32.3	0.34	0.79
0.007−0.088	2b	17 45 58.956	−28 58 34.83	0.40	4.0*	0.43*	1.52*	not detected in Jan. 95		
0.071−0.205	4a	17 46 35.364	−28 58 56.92	0.68	114.1	0.55	1.20	114.1	0.46	1.00
0.079−0.114	4a	17 46 15.377	−28 55 42.52	1.35	51.4	0.21	2.48	-	-	-
0.083+0.064	4a	17 45 34.270	−28 49 55.93	1.45	23.3	0.27	0.92	23.3	0.28	1.17
0.142+0.026	4a	17 45 51.339	−28 48 6.96	0.11	23.9	0.26	1.21	23.9	0.27	0.77

* Measurement of May 1994 (Fig. 1), not detected in either 43 GHz SiO line in Jan. 1995 (Fig. 4).

an H_2O or SiO maser with the "proper" velocity signature (Sect. 3) within this error is considered to be clearly associated with the OH maser. This is the case for 14 H_2O maser sources, and for almost all 18 SiO maser sources.

For the 22 GHz July 1993 observations that are not well calibrated, we allowed an additional 8 sources with a positional difference of twice the synthesized beam size (i.e. an offset of 5″ for July 1993); it might also be possible that the initial position accuracy is actually a bit worse than the claimed 1 to 2″. Larger deviations, up to ∼3 synthesized beams (8″) in July 1993, have been accepted as a detection of an H_2O maser in the OH/IR star for 5 sources with a very high systemic stellar velocity ($|V| > 100$ km s^{-1}). Although we are observing toward the central parsecs of the Galaxy, toward a steep gravitational

potential, it seems unlikely that strong H_2O masers could form in SFR's at these velocities, and in particular at the same time coincide within the position and velocity range of the old, supposedly dynamically relaxed OH/IR star. Finally, another 10 tentative associations are included for which we suggest that the H_2O maser is associated with the OH/IR star. Although they lack sufficient positional coincidence for a definite association, the velocity signature resembles the expected behavior for OH/IR stars enough to be included in the results. Their positional offset from the OH position ranges from 5.″6 to 14.″6. These and other individual associations are commented on in Sect. 4.1.

Using this scheme, we detected 30 (21 + 9 tentative) H_2O maser sources associated with OH masers, and serendipitously 5 H_2O masers in the molecular cloud M−0.13−0.08 in July 1993. In May 1994 we detected 9 H_2O maser sources (8 + 1 tentative association). Among the 5 H_2O masers that we found serendipitously in M−0.13−0.08 in May 1994, 2 of the H_2O masers were also detected in July 1993. We attribute the newly appeared masers between July 1993 and May 1994 in this cloud due to maser variability, which is common in SFR's. Source OH359.956−0.050 (e.g. Sjouwerman & van Langevelde 1996) was serendipitously found as an H_2O maser in both the July 1993 as well as in the May 1994 data. It is an OH/IR star and therefore included in the survey. We discarded all other (possible) detections in the H_2O maser line that we could not associate with either a position or velocity of the targeted OH maser. We did the same to the H_2O masers that were clearly associated with the OH masers in the SFR in Sgr B2.

For the 22 GHz May 1994 and 43 GHz January 1995 observations, we also give the non-detections in Table 5 in cases where we can firmly conclude this. We do not give the non-detections for the July 1993 (over 100 sources) and June 1994 22 GHz observations, and also not for the May and June 1994 43 GHz observations, because many might have been detected if it had been possible to improve the calibration. Positions and spectra measured for many (tentative) associations in these data sets may have very large offsets (on the order of 10″) or improper channel alignment which made clear (spectral) identification difficult. Looking at the data, we suspect that there are a number of H_2O masers (either in OH/IR stars or SFR's) to be found in several of our observed fields, but we lack sufficient sensitivity or calibration to make a definite statement about this. An exception is the field around M−0.13−0.08 as noted above. See also Menten et al. (1997) for additional H_2O masers around Sgr A*, and Sjouwerman et al. (1998b) for newly found OH/IR stars that can be searched for H_2O and SiO masers (Sjouwerman et al., in preparation).

For an impression of the long term variability and the occurrence of multiple maser lines, we list the sources that were detected (denoted with "+") in both our, or other, surveys in Table 6. However, the overlap of the (reliable part of the) data sets is generally small and non-detections, or non-redetections, (denoted with "−") might be due to low sensitivity or variability. Some of the multiple detected sources could provide an opportunity to measure a proper motion of an individual star in the H_2O and SiO maser lines independently.

4.1. Notes on individual H_2O masers

We now compare our detections with the 1612 MHz OH maser detections from our input catalog. In particular, we comment on all tentative associations (Sect. 3.1), and the possible nature of the objects ("SFR" or "OH/IR") that are not obviously OH/IR stars. The non-detections from Lindqvist et al. (1990) in their H_2O survey in a subset of this survey may largely be due, in combination with maser variability, to low sensitivity – their rms is typically 100 to 130 mJy, about a factor of 10 higher than this work.

OH359.429+0.035: tentative association and extrapolated visibility phases. In the 1612 MHz OH maser line, this source has a peculiar OH spectrum from which Lindqvist et al. (1992) could not clearly conclude whether this star is an OH/IR star or connected to a star forming region. With the detection of H_2O maser emission close to the (proposed) stellar velocity, which notably lines up in velocity with the extra central OH peak, we conclude it is most probably a type A H_2O maser of an OH/IR star or a post-AGB star.

OH359.487+0.081: extrapolated visibility phases, which makes the position registration unclear. It is detected three beams away from the OH position, but we conclude it to be a real association, labeled tentative for consistency.

OH359.508+0.179: tentative association and extrapolated visibility phases. Although the H_2O emission is nearly 15″ offset from the OH emission, we do observe 2 H_2O maser peaks in the same line-of-sight with velocities close to the velocity of the two OH peaks, making it, at this high velocity, likely to originate from the same (stellar) source.

OH359.513+0.174: extrapolated visibility phases and within the position to be associated with the OH maser.

OH359.517+0.001: extrapolated visibility phases. Coincident with the OH position and the OH maser velocities. The nature of the absorption profile is unclear.

OH359.712−0.263: detected as a single 1612 MHz OH peak at a velocity of -5 km s^{-1}, but shows the expected H_2O maser profile of an OH/IR star of type A (or A/B) with the systemic velocity close to -17 km s^{-1}.

OH359.751−0.371: also a single peak 1612 MHz OH detection at -8.5 km s^{-1}. The H_2O maser line spectrum resembles spectra of young stellar objects with CO outflows in SFR's (e.g. Genzel & Downes 1977; Felli et al. 1992). However, the source does not show up in the search for compact radio continuum sources (H II regions) by Downes et al. (1979), possibly because it is just outside their surveyed area. Levine et al. (unpublished, E. Schulman, pers. comm.) find H_2O emission at velocities from -82.1 to -66.3 km s^{-1} at this position, supporting the identification with a SFR in this direction.

OH359.783−0.392: association based on the high velocity of the maser.

OH359.837+0.120: OH name and OH position taken from van Langevelde et al. (1992a). A high velocity OH/IR star ($|V_{\rm LSR}| > 250$ km s^{-1}), which also has been confirmed in the 1612 MHz OH line in Sjouwerman et al. (1998b).

All sources around H_2O359.86−0.08: (Table 3, Fig. 3) in this region one finds the dense molecular cloud core M−0.13−0.08,

an ultra compact H II region, and two[3] OH/IR stars. By fitting both OH/IR stars in one beam we happened to point at one of the dense cores of M−0.13−0.08. One of these OH/IR stars (OH359.855−0.078) is detected as an H_2O maser, and with the possible exception of H_2O359.864−0.085 (see next note), all the other H_2O masers found here are likely to be connected to the formation of stars. At least two of these masers had been found previously by Okumura et al. (1989) and in single beam observations by Guesten & Downes (1983) and Lindqvist et al. (1990; note the resemblance with the spectra of Guesten & Downes 1983, and our weak source H_2O359.864−0.084 from our July 1993 observations; it is not to be confused with the strong source H_2O359.865−0.085 in our list). For easy comparison, we show these spectra in Fig. 3 separate from the spectra in Fig. 2. We defer a proper discussion of these detections – together with new observations – in this star forming region to a forthcoming paper.

H_2O359.864−0.085: a possible characteristic double peaked point-like H_2O maser (Table 3; displayed in Fig. 3) which has not been detected in the 1612 MHz OH line by either Lindqvist et al. (1992) or Sjouwerman et al. (1998b). Therefore, we hesitate to classify this object to be an OH/IR star. We cannot exclude that the H_2O emission at 13 km s^{-1} is a side-lobe of H_2O359.861−0.082 in which case this detection would be one of the many SFR's in the direction of M−0.13−0.08. We are more comfortable with a classification as SFR.

OH359.897−0.065: OH name and OH position taken from Te Lintel Hekkert et al. (1989), who quoted OH359.90−0.07 in Habing et al. (1983). Our H_2O position is 6″ off, whereas all our other May 1994 (high resolution A configuration) detections are within about 1″. It is possible that the initial OH position in the catalog is not very accurate, because the Habing et al. (1983) observations were taken in the early days of the VLA. Sjouwerman et al. (1998b) concluded this source is probably not an OH/IR star, because the source has never been confirmed in the 1612 MHz OH line. However, with this H_2O maser detection that matches the velocity of the detection in OH by Habing et al. (1983), and with a line-of-sight velocity of ≈−130 km s^{-1}, this object is probably of stellar origin.

OH359.924−0.034: tentative association because of an offset to the OH position of slightly more than 5″, and because the velocity is just below 100 km s^{-1}.

OH359.936−0.144: seen as a single OH peak or possibly as double or triple 1612 MHz peak by Sjouwerman et al. (1998b), and because it resembles the H_2O maser detection of OH359.751−0.371 we believe also this source has a young stellar origin. Similarly, this source has not been found as a compact continuum source because it is located at the edge of the Downes et al. (1979) survey.

[3] Actually there are three OH/IR stars in this field: OH359.855−0.078, OH359.880−0.087, and OH359.875−0.091. The latter was found in the OH maser line after this survey by Sjouwerman et al. (1998b) with a line-of-sight velocity within the here surveyed region. It is however not detected in the H_2O maser line here, nor in the follow up observations in July 1999 (Sjouwerman et al., in preparation). Its H_2O maser might however been accidentally observed by Lindqvist et al. (1990) as H_2O359.89−0.07, consistent with the OH maser velocity.

OH359.943+0.260: association based on the high velocity of the maser.

OH359.946−0.047: clearly variable in the H_2O maser, because it was not detected in July 93 (with good calibration available because it is in the beam of Sgr A*). Also detected as an H_2O maser by Lindqvist et al. (1990). Publications by a group led by Menten seem not consistent about the observations of this source. In Menten & Reid (1998) the authors indicate to have found H_2O emission from this source by the symbol used in their Fig. 1, but in Menten et al. (1997) the H_2O maser is not mentioned. Also found as SiO maser by others (see references in Table 6).

OH359.956−0.050: OH name and OH position taken from Sjouwerman & van Langevelde (1996). This source was serendipitously found to be an H_2O maser in a single pointing that targeted 5 known OH masers from the survey of Lindqvist et al. (1992). Also found as an H_2O maser by Levine et al. (1995) and Yusef-Zadeh & Mehringer (1995), and as an SiO maser by Izumiura et al. (1998). It is one of the newly found OH/IR stars (Sjouwerman et al. 1998b) and its AGB nature is already extensively discussed in Sjouwerman & van Langevelde (1996) and e.g. Blum et al. (1996).

OH 0.060−0.018: it is the only H_2O maser (except OH359.897−0.065, see above) in the high resolution VLA A-array (set 2a) with more than 1.″25 offset from the OH maser. Its spectrum resembles a type A/B maser, but the offset from the OH maser is large and this tentative association is possibly with an SFR.

OH 0.071−0.205: a bit more offset than 5″ from the targeted OH position, but within 5″ of the position found for the SiO maser found here. Because of its high line-of-sight velocity, we associate this H_2O maser with the OH maser.

OH 0.134−0.023: tentative association because it is a bit further away (6.″3) from the OH maser than our criteria require for a positive association.

OH 0.142+0.026: at an offset of about 14″ to the OH position, it is hard to argue for a type A/B H_2O maser. The velocity coincidence is nevertheless striking, and the association therefore remains tentative.

OH 0.178−0.055: spectrum exactly what one would expect for a type B H_2O maser, but at large offset from the OH maser, and thus a tentative association.

OH 0.190+0.0.036: tentative association; a high velocity source, but with an offset from the OH position larger than 8″.

OH 0.349+0.053: tentative association. An H_2O maser source in the field toward the 1612 MHz OH maser source and close to the H_2O and 1665/1667 MHz mainline OH maser H_2O/OH 0.37+0.04, observed with a single dish (Parkes) by Caswell et al. (1983), and Caswell & Haynes (1983) respectively. The latter do not report 1612 MHz OH maser emission for H_2O/OH 0.37+0.04. However, their detection limit might have been too high. Apart from the position difference, all maser line detections are consistent with an OH/IR star as listed by Lindqvist et al. (1992).

OH 0.543−0.043: found as a multiple peaked H_2O and 1665 MHz OH maser by Mehringer et al. (1993), who classified it as one of the many SFR's in Sgr B1. However, the combination of the double peaked 1612 MHz and 1665 MHz maser

emission and both their and our H_2O maser profile point toward a type I OH/IR star, resolving the issue in favor of the view of Lindqvist et al. (1992).

OH 0.548−0.059: extrapolated visibility phases. Not seen in the H_2O maser line by Mehringer et al. (1993) with good sensitivity, but observed in the 43 GHz SiO maser lines by Shiki et al. (1997). Because of its strong 43 GHz emission and large OH expansion velocity, they suggest that this is a foreground supergiant. Although the source therefore is probably less useful for the proper motion study, it might be very useful for calibration purposes.

OH 0.589−0.108: a high velocity H_2O maser that is probably associated with the OH maser, but because of the extrapolated visibility phases offset by almost 8″.

4.2. Notes on the SiO masers

Of the 16 SiO maser detections in January 1995, 4 had previously been detected in May 1994, whereas 2 SiO maser detections in May 1994 remained undetected in January 1995 (Table 5, Sect. 5.2).

A large fraction of the tentative SiO maser detections (May 1994, Sect. 3.2) were confirmed with emission close to the systemic (stellar) velocity derived from the OH maser profile in January 1995. Striking counter examples are **OH359.977−0.087** and **OH 0.007−0.088**. We are however convinced that they were detected in May 1994 (Fig. 1) and that the derived SiO positions are reliable (better than 1″ within the OH position in May 1994). We note that the former (OH359.98−0.09, Lindqvist et al. 1991) has been detected at 43 GHz previously. We attribute these two non-redetections to the SiO maser variability, which, next to lacking an SiO maser, also may be the case for the two real non-detections.

Sources **OH359.996−0.144** and **OH 0.079−0.114** were only detected in one of the 43 GHz lines. For **OH359.946−0.047** we subtracted a baseline, due to the extended continuum radiation of the Sgr A mini-spiral, before measuring the peak flux and the integrated line flux. Source **OH359.954−0.041** was unintentionally detected in the beam of OH359.952−0.036. Despite the unusual spectra for **OH359.763−0.042** and **OH 0.142+0.026** (which we do not attribute to high noise in the maps; see for comparison some SiO maser spectra in Mira-type stars in Jewell et al. 1991), we conclude that all SiO maser detections originate from the targeted OH/IR stars.

5. Discussion

The high frequency masers found in this survey are useful for follow-up VLBI observations if one has a reasonable chance of detecting them with VLBI arrays; i.e. their positions are well enough determined for the small field of views inherent to VLBI observations (typical 1″), and the maser is strong and stable enough.

Table 5. Non-detections and non-redetections.

May 1994 H_2O maser survey:	
OH359.803−0.021	OH359.946−0.047[b]
OH359.810−0.070	OH359.952−0.036
OH359.855−0.078[a]	OH359.954−0.041
OH359.880−0.087	OH359.955−0.031
OH359.902+0.061	OH359.996−0.144
OH359.939−0.052	OH 0.053−0.062
January 1995 SiO maser survey:	
OH359.873−0.209	OH359.977−0.087[b]
OH359.970−0.049	OH 0.007−0.088[b]

[a] Detected in July 1993. [b] Detected in May 1994.

5.1. Positions

In order to estimate the internal accuracy (i.e. repeatability) of the individual OH/IR star positions, we have compared the positions of the H_2O and SiO masers resulting from this survey with the input catalog, i.e. OH positions from Lindqvist et al. (1992). In the case where Lindqvist et al. (1992) have observed an OH/IR star more than once, usually their positions agree within an arcsecond, occasionally two, and similarly with the positions of e.g. van Langevelde et al. (1993). The Sjouwerman et al. (1998b) OH positions are not of direct use as a starting point for VLBI observations because they are known to deviate from previous catalogs: multiple epochs were aligned with self-calibration, introducing systematic offsets compared to e.g. the Lindqvist et al. (1992) positions of 1.″6, 1.″8 and 4.″2 for their c, b, and a data sets (e.g. Sjouwerman et al. 1998b; Glass et al. 2001; R. Ortiz, pers. comm.). If not stated otherwise, we used the Lindqvist et al. (1992) position with the smallest formal position error, which usually is the one closest to any of the pointing centers and thus suffers the least from sky curvature (see below). Note that the intrinsic size for the H_2O and SiO maser shells, whether they are OH/IR stars or the more massive, larger shell size supergiants, is much less than an arcsecond; for OH/IR stars located at the GC, the SiO shell diameters typically measure 1 mas, and H_2O maser shells are typically a few mas. From astrometric point of view, the higher frequency SiO masers are preferred to measure the stellar positions because of the higher resolution for a given interferometric array, as well as the accuracy to determine the stellar position from the maser position.

Excluding the 2 SFR's, for the H_2O masers associated with the OH/IR stars we find that only 12, 11, and 7 of the positions agree with the original OH maser positions of (mainly) Lindqvist et al. (1992) within 2″, 1.″5, and 1″, respectively. If we assume that the positions coincide because they are close to the true position, and not due to chance alignment or the observing procedure used (see below), the OH and H_2O maser positions only for these 7 to 12 stars thus can be considered to be relatively reasonably determined to the arcsecond level. Actually, a higher accuracy, preferably on sub-arcsecond level, is preferred if we were to use these positions as our starting points in detecting the masers with VLBI. Unfortunately, the

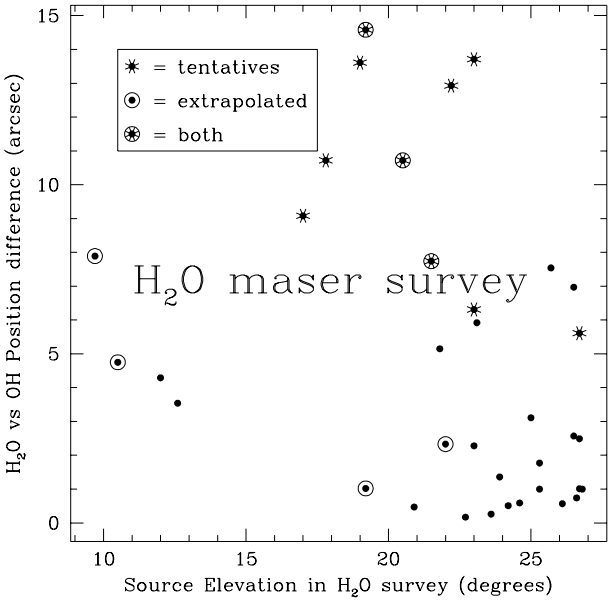

Fig. 5. H_2O maser versus OH maser position difference versus source elevation at observation in the H_2O survey. Starred symbols indicate tentative associations, circled symbols are detections made by extrapolating the visibility phases (i.e. the target scans are not two-sided enclosed by calibrator scans).

quality of most H_2O maser positions does not allow a statement of the internal accuracy of the maser positions.

In Sect. 4 we have reasoned that due to calibration problems, a difference of 5″ between the H_2O and OH maser is acceptable for an association. Associations with larger deviations have been commented on in Sect. 4.1. This implies that at least these H_2O maser positions may not be accurate enough for follow-up VLBI observations; the OH positions may be a better starting point. Although calibration errors are probably the main cause of differing positions, we have investigated whether any systematic biases are apparent. Lindqvist et al. (1992) have measured many tens of OH positions per field (with one field per observing day), whereas we continuously swap fields between our (assumed position of the) phase calibrator, Sgr A*, and our targets. Systematic effects could e.g. depend on distance to the field center due to neglecting 3-dimensional sky curvature in the imaging (for Lindqvist's OH masers), or position of, or distance to the phase calibrator (for the H_2O and SiO masers in this survey). We have not found any systematic effects, even when we account for different observing runs. As the GC culminates at only 27° at the VLA, we show the H_2O versus OH position differences as function of elevation at the time of observation in July 1993 or May 1994 in Fig. 5. We have introduced detections for positional differences of less than 5″, and tentative associations for positional differences of more than 8″. We are not surprised to see more tentative associations at the low end of the observed elevations at about 20°; possible tentative associations at the very low elevations probably already have been discarded by us in an earlier stage due to their larger offsets or phase calibration difficulties.

For the 18 SiO maser sources we find that 10, 15, and 17 of the positions coincide with the OH maser positions within 1″, 1.″5, and 2″, respectively. Only one SiO maser differs more, 2.″4 from the OH maser position, which might originate in the fact that the OH detection of Lindqvist et al. (1992) is weak in the second component, or because the SiO maser position for this source could be measured in the (v = 1) line only (remarkably it is nevertheless within 1″ of the original position given by Winnberg et al. (1985), and about 1.″1 off from the Sjouwerman et al. (1998b) c-position). However, because in general the positions we measure in the (v = 1) and (v = 2) line are coincident on sub-arcsecond level, it is more likely that this relatively large difference between the OH and SiO maser position given for this source is in the fringe of measurement errors. Again, assuming that we are not comparing chance alignments, we conclude that the OH and SiO maser positions for these stars are relatively well determined to the arcsecond level.

Probably the best starting point for follow-up VLBI measurements, without reobserving the sample, is the average of the OH, H_2O and/or SiO maser positions for the masers that independently coincide within 1–2″. Currently, with the OH maser positions of (mainly) Lindqvist et al. (1992) and the H_2O and SiO masers of this work, we can make averages for 12 stellar H_2O masers and 17 stellar SiO masers. Of those, 3 stars agree in positions in all three maser lines (OH359.855−0.078, OH359.946−0.047, and OH359.971−0.119).

5.2. Variability

In contrast to the maser position, which can be improved by observations, the maser variability is of continuous concern for a VLBI campaign; one has to be able to find the source again after a few months or years. Fortunately for stellar objects, OH/IR and other AGB stars, the range in velocity of the maser emission is limited; for the SiO maser within ≈5 km s^{-1} from the systemic velocity. However, the maser flux varies considerably, in particular for the non-saturated H_2O maser. A first impression of variability can be derived by collecting detections and non-detections from previous studies. We have made such an attempt, summarized in Table 6.

A simple count in Table 6 allows us to make a statement about the preferred maser taking into account the maser variability. Of the H_2O masers observed more than once, only about one third is redetected. For the SiO masers, the redetection rate is much higher: 75%. Note that the *re*-detection rate is not dependent on the perhaps subjective selection of the sources (Sect. 3.2), as much of the data is from other observers. Of course this analysis is biased because no correction is made for sensitivity and never reported (mainly non-)detections, but it shows that variability is less of a problem for redetecting a given source in the 43 GHz SiO maser line. For measuring the proper motion on these variable OH/IR stars, the SiO maser also preferred above the less predictable H_2O maser.

6. Conclusions

After excluding two H_2O masers associated with SFR's, for initiating a VLBI campaign we have *stellar* positions consistent *within 1″* between the OH positions of Lindqvist et al. (1992)

Table 6. Multiple and previous detections in OH/IR stars.

Name[a]	Previous/Other		This work[d]	
OH	H_2O[b]	SiO[c]	H_2O	SiO
359.675+0.069	+	+		
359.678−0.024	−	+		
359.762+0.120		+, +[1]		
359.765+0.082			+	+
359.825−0.024	−	+		
359.855−0.078			+, −	+
359.899+0.222	−	+		
359.931−0.063		−, +[2]		
359.946−0.047	+, ±[3]	+[2,3,4,5]	−, +	+, +
359.954−0.041	+	+, +[2,4,5]	−	+
359.956−0.050[d]	+[6,7]	+[2,4,5]	+, +	
359.970−0.049	+[7]	+[5]	−	
359.971−0.119	−	+	+	+
359.974+0.161				+, +
359.977−0.087	−	+		+, −
359.986−0.061	−, +[7]	+		
0.007−0.088				+, −
0.040−0.056	−, +*	+	+	
0.071−0.205	−	+	+	+, +
0.076+0.146	+	−	+	
0.083+0.064				+, +
0.113−0.060	−	+		
0.142+0.026	−	−	*t*	+
0.189+0.052	−	+		
0.543−0.043	+[8]		+	
0.548−0.059	−[8]	+[9]	+	

[a] Lindqvist et al. (1992).
[b] Lindqvist et al. (1990).
[c] Lindqvist et al. (1991).
[d] See Tables 2, 4 and 5.
± See note in Sect. 4.1.
∗ E. Schulman, pers. comm.
t Tentative association.
[1] van Paradijs et al. (1995).
[2] Miyazaki et al. (2001).
[3] Menten et al. (1997).
[4] Izumiura et al. (1998).
[5] Deguchi et al. (2002).
[6] Levine et al. (1995).
[7] Yusef-Zadeh & Mehringer (1995).
[8] Mehringer et al. (1993).
[9] Shiki et al. (1997).

and this survey for 2 H_2O masers, 7 SiO masers, and 3 stellar objects with both H_2O and SiO masers (as well as the OH maser). They will be the best candidates for a proper motion campaign, without the need to find better initial positions. By averaging positions of the different masers that coincide within 1–2″ one may double the number of good starting positions for follow-up VLBI observations. The 43 GHz SiO masers are preferred over the 22 GHz H_2O masers, not only because of the higher angular resolution at which positions can be determined, but also because the SiO maser is more easy to redetect than the H_2O maser. Considering the variability of the sources, this number may be small for statistical analysis, but obtaining several proper motions might provide important information on the *type* of stellar orbits in the GC.

The total number of stellar high frequency masers, thus proper motion candidates, from this survey (excluding tentative associations) is 37: 25 H_2O, and 18 SiO, of which 6 detected in both maser lines. Of the 9 previously reported H_2O masers in OH/IR stars, we observed 7 sources and confirmed 5. We observed 5 of the 17 previously reported SiO masers and confirm all 5. Combined with previous surveys, this totals to about 50 sources (see also references in Table 6). The current maser positions for the latter of these masers may not be accurate enough to detect them instantaneously with VLBI and thus need further astrometric observations.

The masers presented in this paper can be used to measure proper motions in the Galactic center, for example with the new Japanese VERA network, in order to determine the type of orbits and probe the Galactic center gravitational potential.

Serendipitously we have found 8 individual H_2O masers in the molecular cloud M−0.13−0.08 and confirm that the masers found previously by Guesten & Downes (1983) and Okumura et al. (1989) are different masers.

Acknowledgements. In this paper we used observations obtained with the Very Large Array (VLA) of the National Radio Astronomy Observatory (NRAO). NRAO is operated by Associated Universities Inc. under cooperative agreement with the National Science Foundation. For data reduction facilities LOS acknowledges the hospitality of NRAO's Array Operations Center. LOS also acknowledges support for this research by the European Commission under contracts ERBFGECT 950012 and HPRI-CT-1999-00045. The authors also wish to thank the referee, D. Engels, for many helpful suggestions.

References

Blitz, L., Binney, J., Lo, K. Y., Bally, J., & Ho, P. T. P. 1993, Nature, 361, 417
Blum, R. D., Sellgren, K., & Depoy, D. L. 1996, AJ, 112, 1988
Bower, G. C., Backer, D. C., Wright, M., et al. 1997, ApJ, 484, 118
Brand, J., Cesaroni, R., Caselli, P., et al. 1994, A&AS, 103, 541
Caswell, J. L., Batchelor, R. A., Forster, J. R., & Wellington, K. J. 1983, Aust. J. Phys., 36, 401
Caswell, J. L., & Haynes, R. F. 1983, Aust. J. Phys., 36, 361
Comoretto, G., Palagi, F., Cesaroni, R., et al. 1990, A&AS, 84, 179
Deguchi, S., Fujii, T., Miyoshi, M., & Nakashima, J. 2002, PASJ, 54, 61
Downes, D., Goss, W. M., Schwarz, U. J., & Wouterloot, J. G. A. 1979, A&AS, 35, 1
Engels, D., & Lewis, B. M. 1996, A&AS, 116, 117
Engels, D., Schmid-Burgk, J., & Walmsley, C. M. 1986, A&A, 167, 129
Engels, D., Schmid-Burgk, J., & Walmsley, C. M. 1988, A&A, 191, 283
Engels, D., Winnberg, A., Walmsley, C. M., & Brand, J. 1997, A&A, 322, 291
Felli, M., Palagi, F., & Tofani, G. 1992, A&A, 255, 293
Frail, D. A., Diamond, P. J., Cordes, J. M., & van Langevelde, H. J. 1994, ApJ, 427, L43
Genzel, R., & Downes, D. 1977, A&AS, 30, 145
Genzel, R., & Downes, D. 1979, A&A, 72, 234
Genzel, R., Hollenbach, D., & Townes, C. H. 1994, Rep. Progr. Phys., 57, 417
Glass, I. S., Matsumoto, S., Carter, B. S., & Sekiguchi, K. 2001, MNRAS, 321, 77
Guesten, R., & Downes, D. 1983, A&A, 117, 343
Habing, H. J. 1996, A&AR, 7, 97
Habing, H. J., Olnon, F. M., Winnberg, A., Matthews, H. E., & Baud, B. 1983, A&A, 128, 230

Hachisuka, K. 2000, in EVN Symp. 2000, Proc. of the 5th European VLBI Network Symp. held at Chalmers University of Technology, Gothenburg, Sweden, June 29–July 1, 2000, ed. J. E. Conway, A. G. Polatidis, R. S. Booth, & Y. M. Pihlström (published Onsala Space Observatory), 231
Honma, M., Oyama, T., Hachisuka, K., et al. 2000, PASJ, 52, 631
Iben, I. J. 1991, ApJS, 76, 55
Imai, H., Deguchi, S., Fujii, T., et al. 2002, PASJ, 54, L19
Izumiura, H., Deguchi, S., & Fujii, T. 1998, ApJ, 494, L89
Jewell, P. R., Snyder, L. E., Walmsley, C. M., Wilson, T. L., & Gensheimer, P. D. 1991, A&A, 242, 211
Levine, D. A., Figer, D. F., Morris, M., & McLean, I. S. 1995, ApJ, 447, L101
Lindqvist, M., Winnberg, A., & Forster, J. R. 1990, A&A, 229, 165
Lindqvist, M., Winnberg, A., Habing, H. J., & Matthews, H. E. 1992, A&AS, 92, 43
Lindqvist, M., Winnberg, A., Johansson, L. E. B., & Ukita, N. 1991, A&A, 250, 431
Mehringer, D. M., Palmer, P., & Goss, W. M. 1993, ApJ, 402, L69
Menten, K. M., & Reid, M. J. 1998, in IAU Colloq. 164, Radio Emission from Galactic and Extragalactic Compact Sources, ASP Conf. Ser., 144, 229
Menten, K. M., Reid, M. J., Eckart, A., & Genzel, R. 1997, ApJ, 475, L111
Mezger, P. G., Duschl, W. J., & Zylka, R. 1996, A&AR, 7, 289
Miyazaki, A., Deguchi, S., Tsuboi, M., Kasuga, T., & Takano, S. 2001, PASJ, 53, 501
Morris, M., & Serabyn, E. 1996, ARA&A, 34, 645
Nyman, L.-A., Hall, P. J., & Le Bertre, T. 1993, A&A, 280, 551
Nyman, L.-A., Johansson, L. E. B., & Booth, R. S. 1986, A&A, 160, 352
Okumura, S. K., Ishiguro, M., Fomalont, E. B., et al. 1989, ApJ, 347, 240
Olnon, F. M., Winnberg, A., Matthews, H. E., & Schultz, G. V. 1980, A&AS, 42, 119
Reid, M. J. 1993, ARA&A, 31, 345
Reid, M. J., Schneps, M. H., Moran, J. M., et al. 1988, ApJ, 330, 809
Shiki, S., Ohishi, M., & Deguchi, S. 1997, ApJ, 478, 206
Sjouwerman, L. O., & van Langevelde, H. J. 1996, ApJ, 461, L41
Sjouwerman, L. O., van Langevelde, H. J., & Diamond, P. J. 1998a, A&A, 339, 897
Sjouwerman, L. O., van Langevelde, H. J., Winnberg, A., & Habing, H. J. 1998b, A&AS, 128, 35
Te Lintel Hekkert, P., Versteege-Hensel, H. A., Habing, H. J., & Wiertz, M. 1989, A&AS, 78, 399
van Langevelde, H. J., Brown, A. G. A., Lindqvist, M., Habing, H. J., & de Zeeuw, P. T. 1992a, A&A, 261, L17
van Langevelde, H. J., Frail, D. A., Cordes, J. M., & Diamond, P. J. 1992b, ApJ, 396, 686
van Langevelde, H. J., Janssens, A. M., Goss, W. M., Habing, H. J., & Winnberg, A. 1993, A&AS, 101, 109
van Paradijs, J., Spruit, H. C., van Langevelde, H. J., & Waters, L. B. F. M. 1995, A&A, 303, L25
Winnberg, A., Baud, B., Matthews, H. E., Habing, H. J., & Olnon, F. M. 1985, ApJ, 291, L45
Yusef-Zadeh, F., & Mehringer, D. M. 1995, ApJ, 452, L37